Tuning quantum-dot based photonic devices with liquid crystals

Karoline A. Piegdon[1], **Stefan Declair**[1], **Jens Förstner**[1], **Torsten Meier**[1],
Heiner Matthias[2], **Martin Urbanski**[2] **Heinz-S. Kitzerow**[2], **Dirk
Reuter**[3], **Andreas D. Wieck**[3], **Axel Lorke**[4],
and Cedrik Meier[1]*

[1]*Physics Department and CeOPP, University of Paderborn, Warburger Straße 100,
33098 Paderborn, Germany*
[2]*Chemistry Department and CeOPP, University of Paderborn, Warburger Straße 100,
33098 Paderborn, Germany*
[3]*Applied Solid State Physics, Ruhr-University of Bochum, Universitätsstraße 150,
44780 Bochum, Germany*
[4]*Physics Department and CeNIDE, University of Duisburg-Essen, Lotharstr. 1,
47057 Duisburg, Germany*

*cedrik.meier@uni-paderborn.de

Abstract: Microdisks made from GaAs with embedded InAs quantum
dots are immersed in the liquid crystal 4-cyano-4'-pentylbiphenyl (5CB).
The quantum dots serve as emitters feeding the optical modes of the
photonic cavity. By changing temperature, the liquid crystal undergoes a
phase transition from the isotropic to the nematic state, which can be used
as an effective tuning mechanism of the photonic modes of the cavity. In
the nematic state, the uniaxial electrical anisotropy of the liquid crystal
molecules can be exploited for orienting the material in an electric field,
thus externally controlling the birefringence of the material. Using this
effect, an electric field induced tuning of the modes is achieved. Numerical
simulations using the finite-differences time-domain (FDTD) technique
employing an anisotropic dielectric medium allow to understand the
alignment of the liquid crystal molecules on the surface of the microdisk
resonator.

© 2010 Optical Society of America

OCIS codes: (160.3710) Liquid crystals; (160.6000) Semiconductor materials; (230.5750)
Resonators.

References and links

1. K. J. Vahala, "Optical microcavities," Nature **424**, 839-846 (2003).
2. K. Srinivasan and O. Painter, "Optical fiber taper couling and high-resolution wavelength tuning of microdisk resonators at cryogenic temperatures," Appl. Phys. Lett. **90**, 031114 (2007).
3. J. P. Reithmaier, G. Sek, A. Löffler, C. Hofmann, S. Kuhn, S. Reitzenstein, L. V. Keldysh, V. D. Kulakovskii, T. L. Reinecke, and A. Forchel, "Strong coupling in a single quantum dot-semiconductor microcavity system," Nature **432**, 197–200 (2004).
4. T. Yoshie, A. Scherer, J. Hendrickson, G. Khitrova, H. M. Gibbs, G. Rupper, C. Ell, O. B. Shekin, and D. G. Deppe,"Vacuum Rabi splitting with a single quantum dot in a photonic crystal microcavity," Nature **432**, 200–203 (2004).
5. K. Hennessy, A. Badolato, A. Tamboli, P. M. Petroff, E. Hu, M. Atatüre, J. Dreiser, and A. Imamoglu, "Tuning photonic crystal nanocavity modes by wet chemical etching," Appl. Phys. Lett. **87**, 021108 (2005).
6. F. Reinitzer, "Beiträge zur Kenntniss des Cholesterins," Monatshefte für Chemie **9**, 421–441 (1888).
7. K. Busch and S. John, "Liquid-Crystal Photonic-Band-Gap Materials: The Tunable Electromagnetic Vacuum," Phys. Rev. Lett. **83**, 967–970 (1999).

8. Ch. Schuller, F. Klopf, J. P Reithmaier, M. Kamp, and A. Forchel, "Tunable photonic crystals fabricated in III-V semiconductor slab waveguides using infiltrated liquid crystals," Appl. Phys. Lett. **82**, 2767–2769 (2003).

9. G. Mertens, R. B. Wehrspohn, H.-S. Kitzerow, S. Matthias, C. Jamois, and U. Gösele, "Tunable defect mode in a three-dimensional photonic crystal," Appl. Phys. Lett. **87**, 241108 (2005).

10. M. A. Dündar, H. H. J. E. Kicken, A. Yu. Silov, R. Nötzel, F. Karouta, H. W. M. Salemink, and R. W. van der Heijden, "Birefringence-induced mode-dependent tuning of liquid crystal infiltrated InGaAsP photonic crystal nanocavities," Appl. Phys. Lett. **95**, 181111 (2009).

11. S. M. Weiss, H. Ouyang, J. Zhang, and P. M. Fauchet, "Electrical and thermal modulation of silicon photonic bandgap microcavities containing liquid crystals," Opt. Express **13**, 1090–1097 (2005).

12. W. S. Lau, E. F. Chor, S. P. Kek, W. H. bin Abdul Aziz, H. C. Lim, C. H. Heng, and R. Zhao, "The Development of a Highly Selective $KI/I_2/H_2O/H_2SO_4$ Etchant for the Selective Etching of $Al_{0.3}Ga_{0.7}As$ over GaAs," Jpn. J.Appl. Phys. **36**, 3770–3774 (1997).

13. I. C. Khoo and S. T. Wu, *Optics and nonlinear Optics of Liquid Crystals*, (World Scientific Publishing, Singapore, 1993).

14. J. P. Kim, A. M. Sarangan, "Temperature-dependent Sellmeier equation for the refractive index of $Al_xGa_{1x}As$," Opt. Lett. **32**, 536–538 (2007).

15. S. K. Kundu, S. Okudaira, M. Kosuge, N. Shinyshiki, and S. Yagihara, "Broadband dielectric spectroscopy of a nematic liquid crystal in benzene," J. Chem. Phys. **129**, 164509 (2008).

16. A. Taflove, S.C. Hagness, *Computational Electrodynamics* 3rd ed., (Artech House Publishers, Boston, 2005).

17. V. A. Mandelshtam and H. S. Taylor, "Harmonic inversion of time signals and its applications," J. Chem. Phys. **107**, 6756–6769 (1997).

18. V. A. Mandelshtam and H. S. Taylor, "Erratum: Harmonic inversion of time signals and its applications," J. Chem. Phys. **109**, 4128 (1998).

19. J. Li and S.-T. Wu, "Extended Cauchy equations for the refractive indices of liquid crystals," J. Appl. Phys. **95**, 896 (2004).

20. K. Srinivasan and O. Painter, "Mode coupling and cavity-quantum-dot interactions in a fiber-coupled microdisk cavity," Phys. Rev. A **75**, 023814 (2007).

1. Introduction

Tuning photonic resonators [1] is a strong challenge in nanophotonic devices. In a nanolaser, tunability adds another degree of functionality to the device. In quantum information technology, it is often necessary to control the coupling between a semiconductor quantum emitter and the resonant cavity mode. Tunable resonators are also of interest as modulators in communication technology. Different schemes have been applied for tuning photonic cavities, such as material adsorbtion [2] on the device surface, heating the device [3, 4] or defined material removal [5]. All these approaches are limited to low temperatures or lack direct controllability. Here, we report on a room temperature approach for achieving tunability in a photonic resonator with embedded self assembled quantum dots that relies on the interaction of the cavity mode with a liquid crystal. Since their discovery in 1888 by F. Reinitzer [6], liquid crystals have emerged not only due to their interesting physical properties, e.g., their topological features, but also due to their versatility as tools in modern electrooptic devices as well as the display industry. Modern liquid-crystal-based screens make use of the polarization properties. In this letter, we will demonstrate how the optical and electrical anisotropy of nematic liquid crystals can lead to novel device functionality [7]. First steps towards applying liquid crystal technology to photonic structures have been made by Schuller et al. [8]. As the quality factors of these devices were comparably low, the influence of the liquid crystal on the photonic confinement could not be studied in greater detail. Experiments have also been performed in the mid-infrared region [9]. The electrical anisotropy [10, 11] of the liquid crystal molecules enables the use of such kind of structures as a device. In this letter, we will report on a room-temperature device based on self-assembled (In,Ga)As quantum-dots exploiting both the electrical anisotropy and the phase-changing characteristics of the liquid crystal molecules.

2. Experimental

Fabrication of the liquid crystal/semiconductor hybrid devices: As a base material, GaAs-based heterostructures grown by all solid source molecular beam epitaxy (MBE) were used. On a semiinsulating GaAs-substrate, a GaAs buffer layer was deposited. Subsequently, 300 nm of Si-doped GaAs were grown. On top of this layer, a sacrificial layer made of 500 nm $Al_{0.33}Ga_{0.67}As$ was grown, followed by the 240 nm thick membrane layer. In the center of the membrane, a layer of (In,Ga)As-quantum dots was deposited. In order to achieve a high electronic confinement potential, the indium content in these dots is comparably high, leading to a strong photoluminescence signal even at room temperature, where individual orbital shell state can still be observed. Microdisks were formed from the above described base material by contact or electron beam lithography and subsequent isotropic wet etching in a HBr based solution. This step leads to circularly shaped mesa structures, which are subsequently under-etched in a KI-based solution [12]. The radii of the fabricated mirodisks were in the range of $2\,\mu m - 3\,\mu m$. After microdisk fabrication, the devices were optically characterized (see below) and then immersed in the nematic liquid crystal 4-cyano-4'-pentylbiphenyl (5CB). This liquid crystal melts at $T_M = 22.51°C$ and undergoes a nematic-isotropic phase transition at its clearing point of $T_C = 34°C$ [13]. To promote a planar alignment of the liquid crystals on the exposed GaAs surfaces, the samples were pre-treated with either MAP (N-mehtyl-3-aminopropyltrimethoxysilane) or PVA (polyvinyl alcohol). Finally, the devices were either capped with a thin glass slide or – for the electrically controllable devices – using two quartz slides covered with indium tin oxide (ITO) as a transparent conductive electrode. The electrode spacing was $d = 800\,\mu m$ in total.

Spectral response setup: The photoluminescence of the devices was measured in a micro-photoluminescence (μ-PL) setup. As an excitation source, a continuous wave (cw) titanium:sapphire laser was used operating at $\lambda = 780$ nm. The laser light was focused on the sample surface using an infinity-corrected $50\times$-microscope objective with a numerical aperture of NA=0.50 which was simultaneously used to collect the emitted photoluminescence signal. A diffraction limited spot size of $d < 1\,\mu m$ was achieved. The collected PL signal was dispersed in a Czerny-Turner monochromator and detected using an liquid nitrogen cooled (In,Ga)As photodiode array with 512 pixels. The sample temperature was controlled using a temperature sensor and PID control circuit.

3. Discussion and Results

In order to achieve photonic confinement devices with high quality optical modes, microdisk cavities based on GaAs have been fabricated and immersed in the liquid crystal 4-cyano-4'-pentyl-biphenyl (5CB) (details see above).

For characterization of the impact of the liquid crystal immersion on the nanophotonic cavity, the influence of the liquid crystal on the resonant modes of the microdisk devices was checked using photoluminescence (PL) measurements at room temperature (RT). The results are shown in Fig. 1. In the upper part, one can see the PL signal of the (In,Ga)As quantum dots (QDs) at RT before microdisk fabrication. Due to the narrow size distribution of the QD ensemble, even at RT at least the first three excitonic orbital states (*s*-shell, *p*-shell and *d*-shell) are clearly resolved. Fabrication of the microdisk changes the PL spectrum such that the emission is now dominated by the sharp emission peaks of the resonant cavity modes. Depending on the device, spectral linewidths of $\Delta\lambda < 0.3$ nm were measured, corresponding to quality factors of $Q > 4000$. Due to the large pixel size of the (In,Ga)As-detector, this is close to the instrumental limit of the measurement setup. In the lower part of Fig. 1, The PL emission of a microdisk device immersed in liquid crystal is shown. Due to the scattering in the liquid crystal, the excitation laser intensity as well as the PL emission strength is slightly reduced, giving rise to
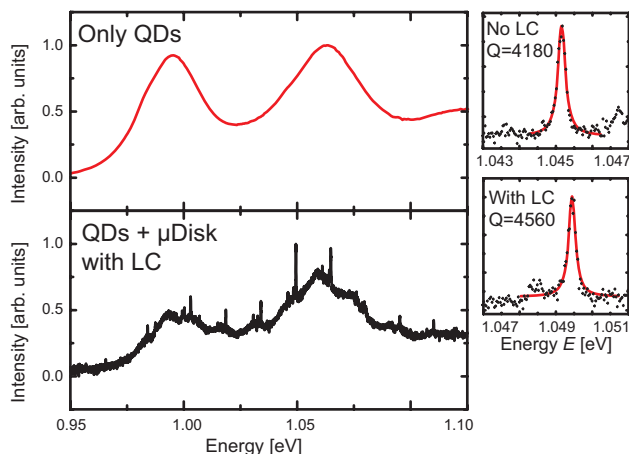
Fig. 1. (Upper part) Room temperature photoluminescence spectrum of the embedded (In,Ga)As quantum layer. The orbital shell structure of the quantum dot ensemble is clearly resolved. (Lower part) PL spectrum of a microdisk sample immersed in the liquid crystal 5CB. The sharp lines decorating the quantum dot emission originate from the fundamental whispering gallery modes in the microdisk. (Right panels) Spectra from two different devices with high quality factors. The maximum achievable quality factor is not signifcantly changed by the immersion.

a noisier signal. The lineshape from two different devices with high quality factors before and after immersion in the liquid crystal is shown in the insets of Fig. 1. As can be seen, in both cases a Lorentzian lineshape is observed with quality factors between 4000 and 5000. Thus, a significant loss of quality cannot be measured for the photonic cavity, which is an important result with respect to the applicability to liquid crystal technology on nanophotonic cavities. The fact that such a reduction in quality factors is not observed is surprising, as the immersion of the microdisk resonator into the liquid crystal reduces the refractive index contrast, which is responsible for the photonic confinement. As a consequence, one expects a redistribution of the electromagnetic field from the semiconductor into the environment, i.e., the liquid crystal. This shows, in contrast to the results obtained by Schuller et al. [8] that liquid crystal technology is indeed compatible with nanophotonic devices. However, the infiltration with the liquid crystal leads to a redshift of the photonic modes due to an increase of the effective refractive index. For the wavelength range of the quantum dot emission around 1 eV, this redshift is around 20 meV.

The nematic liquid crystal adds two degrees of freedom to the newly formed hybrid device: On the one hand, the liquid crystal undergoes a phase transition from the ordered nematic phase to the unordered isotropic phase at the clearing temperature T_C. Therefore, one should expect a strong temperature-induced effect near T_C. On the other hand, due to the dipolar character of the liquid crystal molecules, the material exhibits a strong dielectric anisotropy, leading to the possibility to orient the molecules in an external electric field. As a consequence, the device should respond to an external electric field in the nematic phase.

In the nematic phase, the liquid crystal is birefringent, exhibiting an extraordinary refractive index of $n_{eo} \approx 1.66$ for light polarized with its electric field $\vec{E}$ along the alignment direction $\vec{v}$ of the long molecular axes and $n_o \approx 1.5$ for $\vec{E} \perp \vec{v}$ (at $T = 20°$ C). When fully disordered, the refractive index is isotropic with $n_{iso} = \sqrt{\frac{1}{3}n_{eo}^2 + \frac{2}{3}n_o^2} \approx 1.55$. Therefore, the achievable change of refractive index is quite large in comparison to other systems such as switchable molecules, e.g., azo-benzenes.
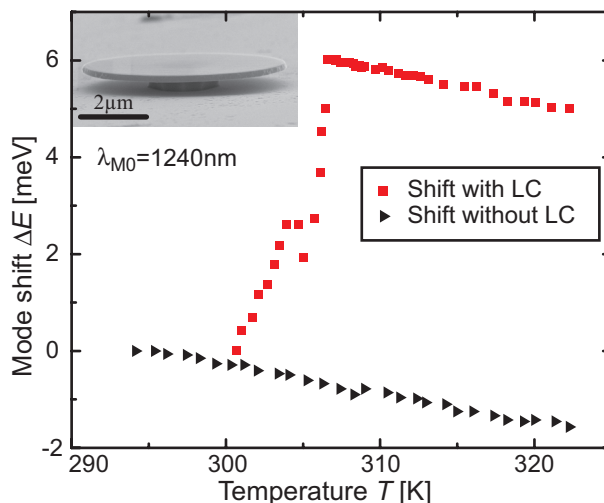
Fig. 2. Temperature dependent tuning behaviour of resonant WGM modes in a liquid crystal immersed microdisk. (Black trace) Reference sample without liquid crystal. The shift is induced by the GaAs thermal lattice expansion. (Red trace) Liquid crystal immersed sample. As the temperature approaches the clearing point $T_C = 307.15\,\mathrm{K}$, the resonant mode energy shifts strongly to higher energies.

The temperature tuning behavior of the liquid crystal immersed devices is shown in Fig. 2. The experiment was conducted as follows: Firstly, the devices were heated above the clearing temperature T_C in order to destroy any pre-ordering. Then, the device was cooled with an applied AC electric field in the $z-$direction. In the next step, the device temperature was increased from room temperature to $T = 323\,\mathrm{K}$. At each temperature, $\mu-$PL spectra were recorded in order to monitor the effect of the dielectric environment on the resonant modes. In the same way, a reference sample was monitored without liquid crystal. The result is shown in Fig. 2. For the reference sample, the resonant mode wavelength shifts to lower energies due to the thermal expansion of the GaAs lattice, leading to a smaller refractive index. The total shift for a temperature change of $\Delta T = 28\,\mathrm{K}$ is about $\Delta E \approx 1\,\mathrm{meV}$. The temperature dependence of the GaAs refractive index can be described using the Sellmeier equation [14], from which we obtain an index change of $\Delta n = 5.7 \times 10^{-3}$. For a resonant cavity mode at $E_M = 1.0\,\mathrm{eV}$, this corresponds to a shift of $\Delta E = -1.67\,\mathrm{meV}$, which is in acceptable agreement with the measurement. In comparison, the liquid crystal immersed device shows a completely different behaviour: Close to the phase transition temperature T_C, the device shows a steep increase of the resonant mode frequency, until a maximum mode shift of about $\Delta E \approx +6.5\,\mathrm{meV}$ is reached. Above the clearing temperature, the resonant mode wavelength is only affected by the effect of the thermal expansion of the semiconductor lattice on the GaAs refractive index, causing a mode shift with the same slope as the reference sample. The effect of the thermal expansion on the geometrical parameters of the resonators such as diameter or membrane thickness is negligible in comparison to the refractive index change.

In the next step, the samples were sandwiched between two transparent electrodes and the response to an external applied electric field in the $z-$direction (epitaxial growth direction) was investigated. In order to prevent electrochemical dissociation of the liquid crystal, an AC-voltage of frequency $f = 50\,\mathrm{Hz}$ was applied. Again, before the experiment the sample was heated above the clearing temperature to remove any remaining order in the liquid crystal molecules and then slowly cooled down to $23°\mathrm{C}$. The results are shown in Fig. 3. As the AC

voltage is increased, the resonant mode frequencies shift to higher energies, until the shift saturates at an applied voltage of 30 V. Considering the device dimensions and the static dielectric constants for GaAs and the liquid crystal [15], one obtains for the saturation voltage an electric field of $E_{\mathrm{GaAs}} = 301.2\,\mathrm{V/cm}$ and $E_{\mathrm{LC}} = 388.6\,\mathrm{V/cm}$, respectively. For the investigated mode at $\lambda_{\mathrm{M,0}} = 1270\,\mathrm{nm}$, the maximum observed shift is $\Delta E \approx 5\,\mathrm{meV}$, which is sufficient for many applications like tunable nanolasers or resonant coupling to narrow emitters such as individual QDs or colloidal nanocrystals.

The temperature effect is fully reversible in the presence of an electric field that leads to an alignment of the LC molecules in the nematic state. The electric field tuning satures once the molecules are fully aligned. However, by shortly heating the sample above the clearing temperature the order is destroyed, and the electric field tuning can be repeated once the sample has cooled down below the clearing temperature again.

The observed frequency shifts in the semiconductor microdisks as a function of the dielectric constant in the environment are caused by the boundary conditions at the disk's interface: The QDs inside the microdisk primarily excite transversal-electric-like (TE-like or even) modes inside the structure due to the strong carrier confinement in the $z-$direction. Thus, in the $z = 0-$plane (center plane of the microdisk slab) the E_z, H_x, H_y-components vanish, while for $z \neq 0$ they need to be considered. When the liquid crystal is in its nematic phase and either fully aligned in-plane or fully out-of-plane, we can describe the liquid crystal using an anisotropic dielectric tensor containing only diagonal elements:

$$\vec{D} = \varepsilon_0 \underline{\underline{\varepsilon_r}} \vec{E} = \varepsilon_0 \cdot \begin{pmatrix} \varepsilon_o & 0 & 0 \\ 0 & \varepsilon_o & 0 \\ 0 & 0 & \varepsilon_{eo} \end{pmatrix} \cdot \vec{E} \tag{1}$$

While the above equation affects the components of the electric field, the magnetic field components are affected by the anisotropic dielectric constant via the time-dependent Maxwell equations, which couple the different field types. However, one needs to answer the question why a change in the dielectric constant in the environment, which supports a continuum of states, can lead to a change of the resonant modes confined in the semiconductor.

To understand the interaction between the resonator and its environment, we consider a plane wave in a dielectric medium with a distinct wave vector $\vec{k}$. A change in the dielectric constant leads to a change in the dispersion $\omega(\vec{k})$, i.e., for a linear isotropic medium, the group velocity $\nabla_{\vec{k}}\omega$ is changed. For the interaction between microdisk and its surrounding, the interface of the disk with the liquid crystal needs to be studied. For a planar infinitely extended interface between semiconductor and liquid crystal, we would argue that we have conservation of $k_{||}$, while $k_\perp$ is not conserved due to the symmetry breaking at the interface. However, for a circularly shaped surface with confined optical modes, i.e., standing waves, we can no longer use $\vec{k}$ as a good quantum number to classify the optical modes of the device. Instead, we have to use the azimutal quantum number m, which is a measure for the number of lobes in the disk periphery. Instead of $k_{||}$ conservation, we can now reasonably argue that the phase of the standing wave inside the disk needs to be matched to the evanescent field in the liquid crystal at the disk/LC interface. This way, when the dispersion in the dielectric environment is changed, in order to preserve phase matching at the interface, the resonant mode frequency inside the device must change as well. This is the reason for the observed resonant mode shifts induced both by temperature and electric field tuning. It should be noted that although TM-like modes are not fed by the QD emission they are still confined, even after immersion of the microdisk with an anisotropic dielectric medium, as can be shown numerically.

In order to understand the anchoring of the liquid crystal molecules on the device surface and their alignment in the electric field, we employed numerical simulations of the resonant mode frequencies. To describe the resonant cavity modes embedded in an anisotropic dielectric
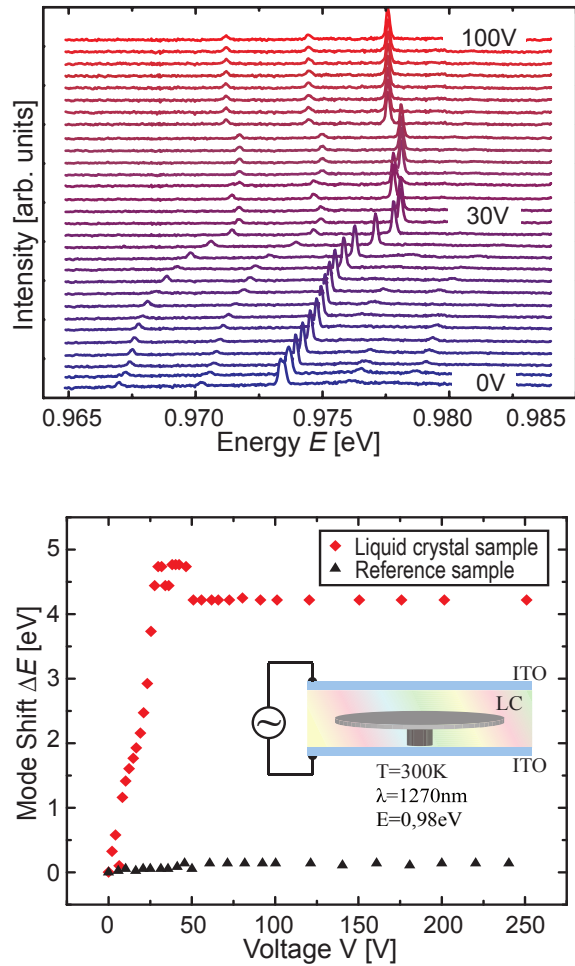
Fig. 3. (Upper part) μ−PL spectra of a microdisk immersed in liquid crystal with an electrical AC field applied perpendicular to the disk plane. (Lower part) Tuning behaviour of a resonant cavity mode as a function of the applied voltage.

environment, an in-house developed finite-difference time-domain code with standard CPML "open" boundaries and subcell accuracy borrowed from Finite Integration Technique (FIT) was used (FDTD, [16]) to simulate the light field propagation after excitation with an ultrashort broadband pulse. A magnetic dipole was used in order to excite the TE-like modes of the semiconductor cavity. The MIT "Harminv" software package based on the filter diagonalization method [17,18] was used to efficiently extract the frequency and decay rate of the cavity modes from the simulated electric fields.

In our simulations, a dimensionless parameter o was introduced in order to accomodate for the different orientations of the liquid crystal molecules. A value of $o = -1$ corresponds to parallel ordering of the molecules, i.e., the molecules are oriented in the xy−plane, while a value of $o = +1$ means that the molecules are fully aligned along the z−axis, corresponding to $\varepsilon_{eo} = \varepsilon_{zz}$. For $-1 < o < +1$, the effective dielectric constant $\underline{\underline{\varepsilon}}_r$ is linearly interpolated, assuming that the dielectric tensor contains only diagonal elements, which is a requirement of the used algorithm. In this (simple) approximation we neglect the temperature dependence [19] of the refractive
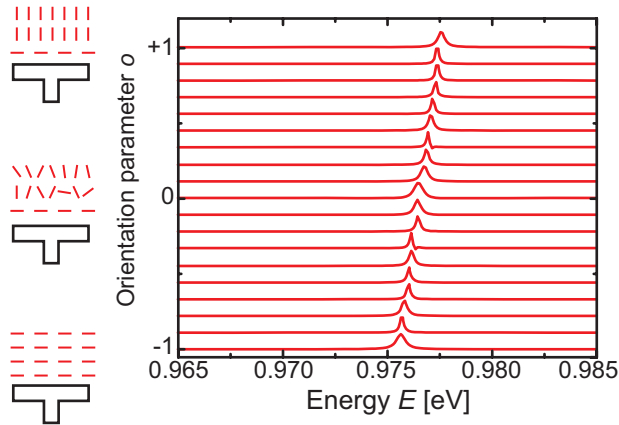
Fig. 4. FDTD simulation for different orientations of the liquid crystal molecules. The vertical axis describes the alignment of the molecules, where $S = 1$ corresponds to vertical alignment, $S = 0$ to an intermediate partially disordered state and $S = -1$ to parallel alignment in the disk plane.

index of the liquid crystal, as we are mostly interested in the electric field induced alignment. Thus, it is assumed that the microdisk environment is uniaxially birefringent with the optical axis perpendicular to the disk plane. This assumption describes the case of vertical alignmen ($o = +1$) and the isotropic state ($o = 0$) correctly, but for planar alignment, this symmetry requires a uniform distribution of the local alignment direction over all azimuthal angles. The results of the calculation are shown in Fig. 4. Here, the frequency of a single resonant mode was isolated and its shift was tracked as the orientation of the liquid crystal molecules were changed. For a full orientation of the liquid crystal molecules in the xy-plane ($o = -1$), one obtains the lowest mode frequency. As the orientation parameter is increased towards $o = 0$, the frequency increases linearly with the orientation parameter o. As the orientation is changed into the z-direction, the resonant mode frequency is further increased up to a maximum value for the vertical alignment ($o = +1$). The comparison with experiment (Fig. 3) suggests that the final orientation of the liquid crystal molecules is indeed vertical as it is assumed in the calculation. However, before the electric field is applied, it is not clear whether the pretreatment (see method section) of the GaAs surface leads to a planar alignment of the LC molecules, or if it has no effect at all.

For the three extreme cases, i.e., in-plane alignment, partial disorder and vertical alignment, we obtain resonant mode energies of $E(o = -1) = 0.9754\,\text{eV}$, $E(o = 0) = 0.9766\,\text{eV}$ and $E(o = +1) = 0.97769\,\text{eV}$ for the traced mode. This means, if one assumes that the LC molecules were disordered before the experiment, i.e., the pretreatment of the GaAs surface would only have had a negligible effect on the orientation, one would expect a shift from isotropic to vertical alignment of $\Delta E = 1.2\,\text{meV}$, which is far below the experimentally observed shift of more than $\Delta E = 5\,\text{meV}$. If one assumes that the pretreatment of the GaAs surface has lead to an in-plane alignment corresponding to the case $o = -1$ before the electric field was applied, one obtains from the calculations an effective shift of $\Delta E = 2.3\,\text{meV}$. While this is much closer to the experimentally observed result, there is still a significant discrepancy. The most likely explanation for this difference is the existence of fabrication imperfections which lead to scattering at the interface and therefore to an increased leaking of confined optical modes in the environment of the disk, where they can interact with the liquid crystal molecules. While in reality such fabrication imperfections cannot completely be avoided, the idealized dielectric

structure assumed in the calculations is only limited by the computational grid. Moreover, additional numerical calculations suggest that also an excentricity of the microdisk as well as a non-cylindrical edge profile as described by Srinivasan and Painter can explain the quantitative difference [20].

4. Conclusion

In conclusion, we have shown that liquid crystal technology can be applied to photonic cavity devices. Liquid crystals are indeed a very versatile tool, as they respond to many external parameters, such as temperature or external electric field as shown in this letter. In fact, due to the richness of this material class, possible applications go far beyond the experiments shown here, where a comparably simple liquid crystal molecule was chosen. By choosing the molecule, devices can be realized that are custom designed for specific applications, such as high switching speed, temperature window of operation etc.